IEEE Access
Multidisciplinary | Rapid Review | Open Access Journal

Received January 27, 2020, accepted February 8, 2020, date of publication February 13, 2020, date of current version February 26, 2020.

Digital Object Identifier 10.1109/ACCESS.2020.2973665

Quantification of Acrylonitrile Butadiene Styrene Odor Intensity Based on a Novel Odor Assessment System With a Sensor Array

HONG MEN, CHONGBO YIN, YAN SHI, XIAOTONG LIU, HAIRUI FANG, XIAOJU HAN, AND JINGJING LIU

School of Automation Engineering, Northeast Electric Power University, Jilin 132012, China

Corresponding authors: Hong Men (menhong@neepu.edu.cn) and Jingjing Liu (liujjtiger1986@sina.com)

This work was supported in part by the National Natural Science Foundation of China under Grant 31772059 and Grant 31871882, in part by the Key Science and Technology Project of Jilin Province under Grant 20170204004SF, in part by the Provincial Special Funds for Industrial Innovation of Jilin Province under Grant 2018C034-8, and in part by the Science and Technology Development Plan Project of Jilin under Grant 201750233.

ABSTRACT As an engineering plastic, acrylonitrile butadiene styrene (ABS) has been widely used in the automobile trims. The odor intensity of ABS can be considered as an important reference for the quality of in-vehicle air. Currently, many automobile manufacturers employ their own testing methods to measure the odor intensity of the trims. Different rules lead that the market lacks a unified standard to evaluate the odor intensity. In this paper, a novel odor evaluation system was proposed to measure the odor intensity of ABS. According to coefficient of variation (CV), analysis of variance (ANOVA), and principal component analysis (PCA), eight sensors were selected to compose an array with stability, repeatability, and selectivity. By means of the pretreatment and the feature extraction, the odor features were quantified by grey relation analysis (GRA). Then, the regression models were constructed by extreme learning machine (ELM), random forest (RF), and support vector machine (SVM) to predict the odor intensity. The results indicated that the quantified data could describe the odor intensity accurately and be predicted well by three models. This study demonstrated that the system achieved perception and quantification of the odor intensity of ABS. In conclusion, a self-developed system was put forward, offering a new technique to evaluate the odor intensity, prospective to replace the manual testing.

INDEX TERMS Acrylonitrile butadiene styrene, odor evaluation system, odor intensity, sensor array.

I. INTRODUCTION

With the development of automobile industry, the quality of in-vehicle air is getting more and more attention [1]. Despite people spend limited time in vehicles, the high concentration of pollutants in this microenvironment account for a large proportion of air pollutants [2]. For a nonsmoker, about 10-60 % of entire contaminants root in the exposure to vehicles [3]. The poisonous contaminants will endanger human health directly, leading to a series of diseases, such as allergic rhinitis, asthma, and even leukemia [4]. At present, pollution of in-vehicle air, hypertension, and AIDS have been listed as three threats to the human health by World Health Organization [5].

The associate editor coordinating the review of this manuscript and approving it for publication was Baozhen Yao.

The volatile contaminants release from the instrument panels, the door planks, the steering wheels, et al [6], [7]. Since favorable performances and lower cost, acrylonitrile butadiene styrene (ABS) is employed to process the automobile trims [8]–[10]. However, some monomers and emulsions may be remained during the course of polymerization, resulting in the diffusion of the irritant gases [10]. Besides, the trims are shaped from the master batches of ABS with high temperature and pressure. The materials release more volatile organic compounds (VOCs) when vehicles are exposed to the burning sun [6], [11]. At last, the pigments used for painting the trims emit the aromas of benzene series, and injure the respiratory tract and the skin under prolonged exposure to vehicles' microenvironment [11].

At present, the traditional physical and chemical analyses measure the odor intensity by detecting the concentrations

of substances. However, there are some inevitable disadvantages. For instance, the colorimetry [12] is a suboptimal choice in long sampling period and slow response, and the electrochemical analysis [13] depends on strict operation environment. Despite the comprehensive two-dimensional gas chromatography [14] shows enhanced selectivity and improved sensitivity for the samples, the preparation of dirty samples is inevitable [15]. In conclusion, the traditional analysis methods ignore the measurement of comprehensive odor intensity. Consequently, auto manufacturers employ respective experts to test the odor intensity of automobile plastics. For example, Volkswagen heats and preserves the samples according to different temperatures and time. And the odor intensity is divided into six grades [16]. Nevertheless, General Motors utilizes the higher temperature to heat the samples and divide the odor intensity into ten grades [17]. Relative to above companies, TOYOTA detects the smells of parts from various regions and divides the odor intensity into six grades, from zero to five [18]. The detailed techniques and evaluation criteria are shown in Table 1. For different auto manufacturers, the pretreatment and grades of materials are inconsistent, but the manual testing is the main method to measure the odor intensity of ABS. Here, the test methods and evaluation criteria of three manufacturers are just listed. Despite artificial sensory evaluation is direct to sense the odor intensity [19], but causes damage to the health of the valuators working for a long time. Moreover, the valuators are probably affected by various factors, such as subjective preferences, working condition, and physical health [7], [20]. Above all, the automobile manufacturers and part plants employ their own valuators to measure the odor intensity of the same product, which gives rise to disputes for the quality of product. Simultaneously, different automobile manufacturers arise distinctions for the odor intensity, resulting in the lack of a unified standard in the whole market.

TABLE 1. The test methods and evaluation criteria of three companies.

Auto Manufacturers	Pretreatment	Grades	Evaluation Criterion
Volkswagen	Wetness (23 ± 2 °C), (24 ± 1 h) Wetness (40 ± 2 °C), (24 ± 1 h) Dryness (80 ± 2 °C), 2 h ± 10 min	6	1 not perceptible 2 perceptible, not disturbing 3 clearly perceptible, but not disturbing 4 disturbing 5 strongly disturbing 6 not acceptable
General Motors	Wetness (40 ± 2 °C), (24 ± 1 h) Wetness (70 ± 3 °C), (24 ± 1 h) Dryness (105 ± 3 °C), 2 h ± 10 min	10	1 Intolerable 2 Severe 3 Annoying 4 Objectionable 5 Borderline tolerable 6 Tolerable 7 Clearly noticeable, but not objectional 8 Noticeable, trace 9 Just noticeable 10 Odorless
TOYOTA	Direct irradiated parts: (80 ± 2 °C), 1 h Not direct irradiated parts: (60 ± 2 °C), 1 h Instrument panel, Awning, Packing tray: (100 ± 2 °C), 1h	6	0 Odorless 1 Weaker than standard odor (almost unrecognizable) 2 A little weaker than standard odor (slightly recognizable) 3 As strong as the standard odor (Easily recognizable) 4 A little stronger than standard odor 5 Stronger than standard odor

The olfactory bionic technology applies gas sensor arrays [21], [22] to simulate the signals produced by olfactory cells, and combines with advanced recognition methods [23], [24]. The thin film on the sensor surface makes full contact and interaction (including physical adsorption, chemical adsorption, even chemical reaction) with the gases, and the electrical signals can be converted from chemical information [25]. Besides high accurateness and rapid responses, the sensors need to consider the cross sensitivity in the construction of the sensor array [26]. Szulczyński *et al.* [27] employed an electronic nose based on eight gas sensors to recognize the interaction of several components in the gas and surveyed the ingredients of the contaminants. On the other hand, the pattern recognition methods are employed to classify the signals representing the smell features. Osowski and Siwek [28] utilized the electronic nose to identify the distorted data of biological additives in the gasoline by means of principal component analysis (PCA), wavelet transform, support vector machine (SVM), etc., summing up the advantages of SVM in reducing errors. In the past few years, the olfactory bionic technology has progressed in the evaluation of the grades of paraffin [29], air quality [30], and the flavors of beverage [31]–[33].

This study proposed an odor evaluation system designed with a sampling device, a sensor array, and an analysis software to measure the odor intensity of four kinds of ABS. In order to construct the sensor array, coefficient of variation analysis (CV), analysis of variance (ANOVA), and PCA were applied to select the sensors with stability, repeatability, and selectivity. The features were extracted from the data obtained in the stable state. Then, grey relation analysis (GRA) [34] was implemented to quantify the odor intensity. Finally, the regression models were established by means of extreme learning machine (ELM), random forest (RF), and SVM to predict the quantified values of unknown samples. And the quantified values have a good performance in the training sets ($R^2 > 0.91$) and test sets ($R^2 > 0.88$). In conclusion, the odor

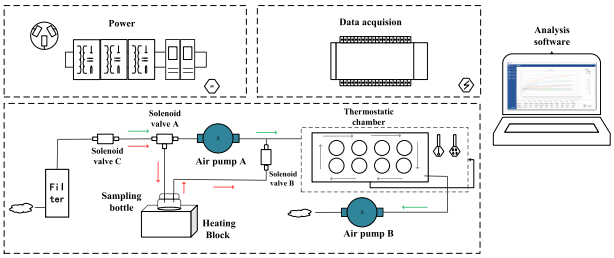

FIGURE 1. The schematic diagram of the ABS odor evaluation system.

intensity of ABS detected by the odor evaluation system was described in terms of the accurate numbers, rather than rough grades. Therefore, the self-developed evaluation system provided a novel technique to measure the odor intensity of ABS, promising to unify the odor evaluation criteria.

II. MATERIALS AND EXPERIMENT

A. SAMPLES PREPARATION

In this study, four kinds of ABS with the same grade were purchased from Qi Mei Company (a manufacturer of ABS), which were high heat-resistant ABS, heat-resistant ABS, flame-retardant ABS, and polypropylene and glass ABS. Different ABS brands were stored in distinct storage bags to avoid pollution from other smells. Additionally, the disposable gloves were required to be worn before sampling.

To begin with, weigh the particles of ABS according to 10g, 20g, 30g, 40g, and 50g. Then, the samples were placed in bottles with 200 ml and sealed with lids. Eighty tests were implemented for each kind of ABS (e.g. Brand high heat-resistant ABS: 10g × 16, 20g × 16, 30g × 16, 40g × 16, 50g × 16), and a sum of 320 samples could be obtained. After sampling, the bottles were preserved in a cool and dry environment.

B. DESIGN OF ABS ODOR EVALUATION SYSTEM

1) ABS ODOR EVALUATION SYSTEM

The odor evaluation system consisted of a sampling device, a sensor array, and an analysis software. The whole construction of the system is shown in Fig. 1. And Fig. 2 shows the photograph of the whole system and the interior detection device.

The sampling device was designed in accordance with dynamic headspace sampling, including an air generator and a thermostatic heater. The air generator provided pressure for the circulation of the gases, where the active carbon was used to wipe off the vapors and the impurities from air. The thermostatic heater was employed to generate the volatile gases by heating the particles of ABS at 40 °C.

As for the gas chamber, made up of poly tetra fluoroethylene (PTFE), a synthetic polymer material that is insoluble in almost all organic solvents. The structure of the gas chamber is shown in Fig. 2 (b). The sensor array was integrated by ten sensors. In this paper, eight sensors were applied to detect the odors, which were MQ-2, MQ-3, MQ-137, TGS-813, TGS-821, TGS-825, TGS-830, and TGS-2610, selected from Table 2. The valves and pumps were applied to control the cleaning of the gas circuit and gas chamber. The EM936M (a data acquisition card) collected the multi-channel sensor response signals and converted the analog signals into digital signals. At last, the signals were transmitted to a PC.

TABLE 2. The characteristics of the sensors.

No.	Sensors	Concentration Range(ppm)	Sensitive Gases
1	MQ-2	300-10000	Liquefied Gas, natural gas
2	MQ-3	10-1000	Ethanol
3	MQ-135	10-1000	NH_3, benzene vapor
4	MQ-137	5-500	NH_3
5	MQ-138	5-500	Toluene, acetone, ethanol, H_2
6	TGS-831	10-300	R-21, R-22
7	TGS-813	500-10000	Alkanes, ethanol
8	TGS-821	30-1000	H_2
9	TGS-822	50-5000	Benzene, toluene, ethane
10	TGS-825	5-100	H_2S
11	TGS-830	100-3000	R22
12	TGS-832	100-3000	R-134a
13	TGS-861	30-300	Ammonia, amines
14	TGS-2610	500-10000	Butane, LPG
15	TGS-2611	500-10000	CH_4, natural gas
16	2m009	0-500	Toluene

The analysis software was compiled on C programming language to accomplish the start-up of the equipment, and the data communication and storage. At the same time, the implanted MATLAB software was implemented to complete the pre-processing and the feature extraction of raw data, and quantify the odor intensity.

2) SENSORS SELECTION

In the construction of the sensor array, the sensors were supposed to be selected with stability, repeatability, and selectivity when responding to the gases. On the other hand, the high-dimensional data may result in the redundant features. Thus, based on four finds of ABS, the steps of selecting the sensors are as follows:

a: COEFFICIENT OF VARIATION

CV, a statistic method, can reflect the variation of the observed values. The variation is becoming weaker with the decrease in CV. Also, CV reflects the stability of the sensors [35]. Namely, the larger CV, the worse stability [36]. Table 3 describes the CV of sixteen sensors. It can be

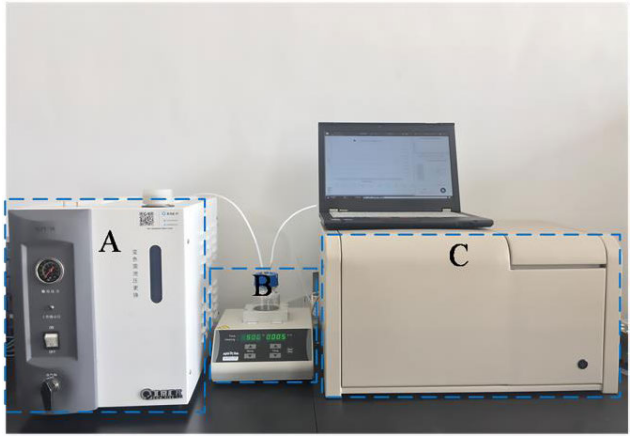

(a)

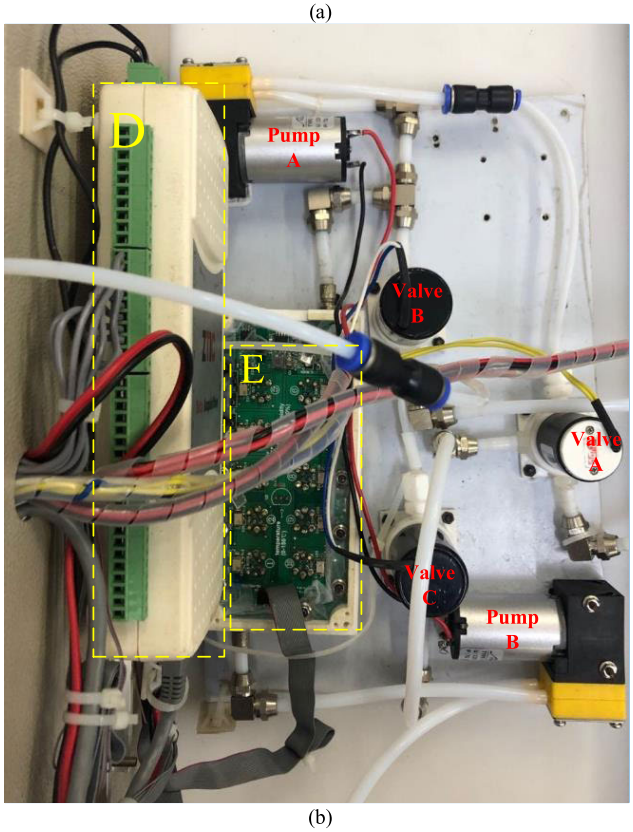

(b)

FIGURE 2. Photograph of the practical ABS odor evaluation system and the interior detection device: (a) Photograph of the practical ABS odor evaluation system. Part A is an air generator with a filter, part B is a thermostatic heater with a sampling bottle, and part C is a detection device which involves a sensor array, a data acquisition card, two pumps, and three valves. (b) Photograph of the interior detection device. Part D is the data acquisition card and part E is the sensor array.

acknowledged that the variable coefficients of MQ-138, TGS-822, and TGS-861 were more than that of others. Thus, these three sensors were excluded due to the worse stability.

b: ANALYSIS OF VARIANCE

As a means of hypothesis test, ANOVA mainly makes statistical analysis for many relevant factors, and compares the random errors and the systematic errors. In this paper, each sensor was served as a factor, and the changes of voltage values were checked through ANOVA. In general, the repeatability of the sensors is becoming better with the decrease in intra-class quadratic mean. The larger F value or the less p value means the preferable discrimination of the sensors. Table 4 describes the ANOVA of sixteen sensors.

TABLE 3. The coefficient of variation of the sensors.

No.	Sensors	Coefficient of Variation
1	MQ-2	0.1496
2	MQ-3	0.1383
3	MQ-135	0.1583
4	MQ-137	0.1562
5	MQ-138	0.6667
6	TGS-831	0.1242
7	TGS-813	0.1259
8	TGS-821	0.2096
9	TGS-822	0.6355
10	TGS-825	0.1761
11	TGS-830	0.0272
12	TGS-832	0.1499
13	TGS-861	0.5813
14	TGS-2610	0.2676
15	TGS-2611	0.3796
16	2m009	0.3350

TABLE 4. The analysis of variance of the sensors.

No.	Sensors	Intra-class Quadratic Mean (%)	F Value	P Value
1	MQ-2	0.036	21.13	< 0.0001
2	MQ-3	0.13	26.12	< 0.0001
3	MQ-135	2.085	18.08	0.065
4	MQ-137	0.371	6.13	< 0.0001
5	MQ-138	1.256	93.55	< 0.0001
6	TGS-831	0.056	12.22	0.031
7	TGS-813	0.006	7.27	0.0121
8	TGS-821	0.031	6.34	0.0017
9	TGS-822	0.033	1.21	0.021
10	TGS-825	0.076	9.23	< 0.0001
11	TGS-830	0.0021	1.96	< 0.0001
12	TGS-832	0.066	1.61	0.221
13	TGS-861	0.058	2.56	< 0.0001
14	TGS-2610	0.073	15.42	< 0.0001
15	TGS-2611	0.035	1.75	< 0.0001
16	2m009	0.005	14.56	0.035

TABLE 5. The coefficient of the first two principal components.

No.	Sensors	The Coefficient of Principal Component	
		The Coefficient of PC1	The Coefficient of PC2
1	MQ-2	-0.04	0.36
2	MQ-3	0.27	0.34
3	MQ-135	0.27	-0.13
4	MQ-137	0.28	-0.36
5	MQ-138	-0.02	-0.13
6	TGS-831	0.29	-0.19
7	TGS-813	0.27	0.31
8	TGS-821	0.27	-0.21
9	TGS-822	0.21	0.20
10	TGS-825	0.24	0.25
11	TGS-830	0.13	0.30
12	TGS-832	0.20	0.22
13	TGS-861	0.28	0.26
14	TGS-2610	0.22	0.20
15	TGS-2611	0.23	-0.14
16	2m009	0.22	0.12

As shown in Table 4, the mean square values of MQ-135 and MQ-138 were more than that of others, meaning that these two sensors with the poorer repeatability. Moreover, the p value of TGS-832 was much higher than that of others. With the above analysis, MQ-135, MQ-138, and TGS-832 were deleted from the sensor array.

c: PRINCIPAL COMPONENT ANALYSIS

As a multivariate statistical means, PCA is able to transform the initial data into linearly independent characteristic components, and retain most of the information of the original data. When the cumulative contribution rates in PCA are more than 80%, the coefficient of PC2 can indicate the selectivity of the sensors. Namely, the greater coefficient of PC2, the preferable selectivity. In this study, the cumulative contribution rates of the three principal components were 87.12%. As shown in Table 5, the coefficients of PC2 of MQ-135, MQ-138, TGS-831, TGS-2611, and 2m009 were less than that of others, which proved that these five sensors were provided with the worse selectivity.

In conclusion, MQ-2, MQ-3, MQ-137, TGS-813, TGS-821, TGS-825, TGS-830, and TGS-2610 were determined to constitute the final sensor array.

C. EXPERIMENT APPROACHES

To begin with, the ambient temperature and humidity were at 20 ± 2 °C and 65 ± 5 % RH. Before measuring, open the equipment and the software interface to preheat the gas sensors for 1 h until the sensors reach steady voltage values. The formal operations are as follows:

(1) Define the file names in the light of the experimental requirements (manufacturers xx, model number xx) and save the files in the specified path.
(2) The cleaning of gas circuit contains three steps. First of all, open valve C to allow the pure air from air generator to flow into the conduit. After that, open valve A and close valve B and all pumps to wash the left conduit for 5 s. Then, keep valve A and valve C on and open valve B and pump A to wash the right conduit for 10 s.
(3) After cleaning the gas circuit, keep valve A, valve C, and pump A on. Close valve B and open pump B to clean the chamber until the sensors' signals recovered their own baseline values. The whole cleaning lasted 300 s with a flow rate of 1.2 L/min.
(4) Set the heater at 40 °C and place the prepared samples into the heater for 30 min. Afterwards, keep valve A on, close valve C and pump A, and open valve B. Then, a sample injection needle was inserted into the bottle, and the headspace gases gradually entered the gas chamber and reacted with the sensors in 180 s. Fig. 3 shows the voltage responses of four sorts of ABS.
(5) Pull out the injection needle and finish this test. Steps (1) – (4) were repeated to start next test.

It is well known that the response values of the sensors are sensitive to the environment. Consequently, the response values could be acquired by eliminating the baseline values. The response values were calculated by the following formula:

$$X_i = X_s - X_b \tag{1}$$

where, X_s is the measured value, and X_b is the baseline value. To reduce the differences between the data and improve the convergence rate, the response values were supposed to be normalized. The min-max normalization formula is as follows:

$$x_i = \frac{X_i - X^{\min}}{X^{\max} - X^{\min}} \tag{2}$$

where, $X^{\max}$ and $X^{\min}$ are the maximum and minimum values of the response values, respectively. And the final normalization between [0, 1] was gained.

As shown in Fig. 3, the sensors kept the initial values before contacting with the gases. After 5 s, the voltage response of each sensor raised fast and held a stable value at about 120 s. Therefore, the average value of each voltage response curve from 120 s to 139 s was obtained as the feature. There were four sorts of ABS, and four groups of 80 × 8 feature matrices could be gained.

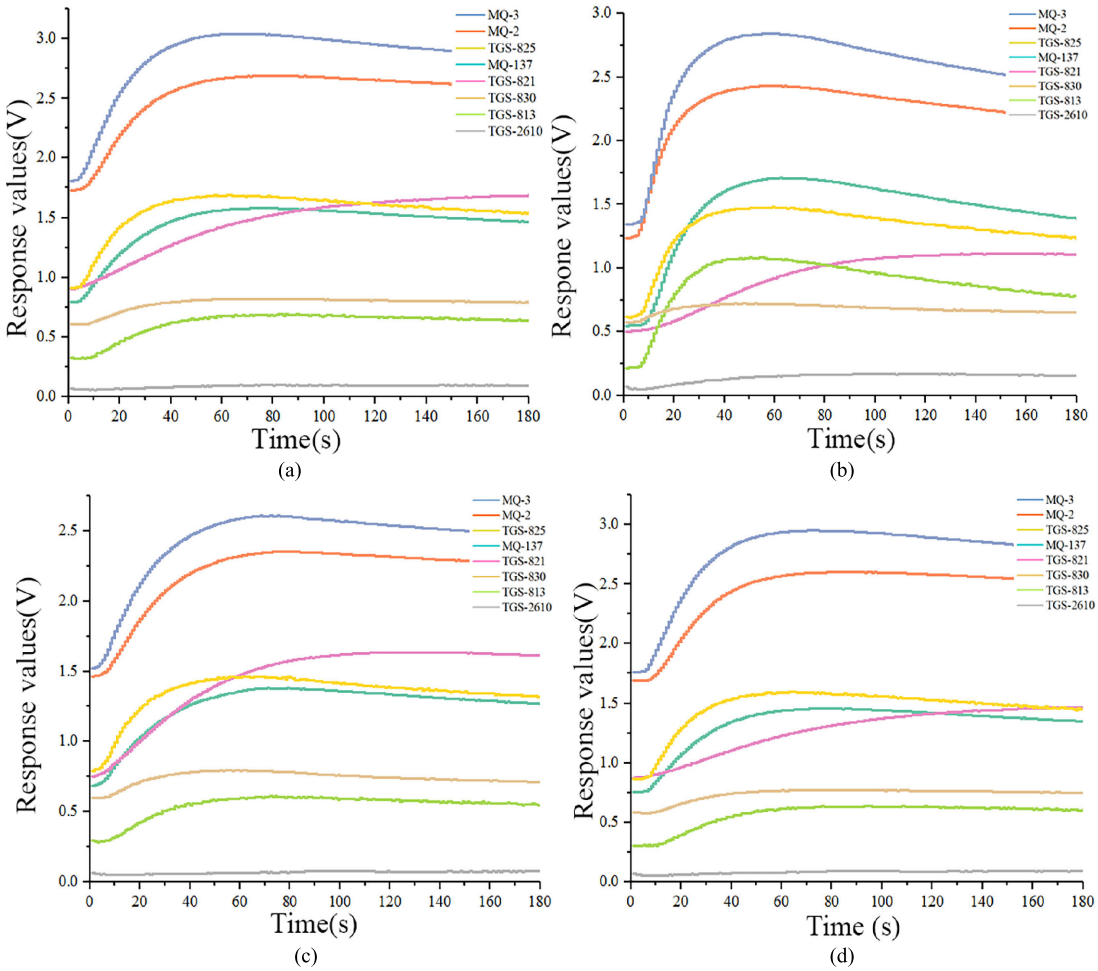

FIGURE 3. The voltage responses of four sorts of ABS: (a) High heat-resistant ABS, (b) Heat-resistant ABS, (c) Flame-retardant ABS, (d) Polypropylene and glass ABS.

III. RESEARCH METHODS

A. GREY RELATION ANALYSIS

GRA is a method to analyze the correlation of various factors in the system, developed by Deng Julong [37]. The contribution of each factor to the system can be concluded based on the grey relational degree. The geometric similarity of the data sequence of each factor is studied to determine the correlation between the factors [38]. The closer the geometry is, the greater the correlation is. Because of good universality and reliability, GRA makes progresses in mathematics and economics [39]. The particular approaches are as follows:

(1) Determine the referred sequence and the compared sequence. Suppose there are n evaluation indexes and m evaluation objects. Hence, the referred sequence could be described as: $x_0 = \{x_0(k)|k = 1, 2, \ldots, n\}$, and the compared sequence could be described as: $x_i = \{x_i(k)|k = 1, 2, \ldots, n; i = 1, 2, \ldots, m\}$.

(2) The weight of each index is determined as: $\omega_k = [\omega_1, \omega_2, \ldots, \omega_n]$.

(3) The correlation coefficient is obtained by solving the following problem:

$$\zeta_i(k) = \frac{\min\limits_i \min\limits_k |x_0(k) - x_i(k)| + \rho \max\limits_i \max\limits_k |x_0(k) - x_i(k)|}{|x_0(k) - x_i(k)| + \rho \max\limits_i \max\limits_k |x_0(k) - x_i(k)|}, \quad k = 1, 2, \ldots, n \tag{3}$$

where ρ is the discrimination coefficient ($0 < \rho < 1$), usually recommended to be 0.5.

(4) Finally, the correlation r_i can be obtained from Equation (4):

$$r_i = \sum_{k=1}^{n} \omega_k \zeta_i(k) \tag{4}$$

B. EXTREME LEARNING MACHINE

ELM is a machine learning algorithm based on feedforward neural network, developed by Huang Guangbin [40]. Compared to the other networks, ELM sets the random weights (ω) and thresholds (b) of the hidden layer without adjustment,

which reduces computation [41]. The output weights (β) are determined by the activation function and the amount of hidden layer neurons. Owe to the higher efficiency and the stronger generalization, ELM has an extensive application in classification and regression [42]. The detailed steps are as follows:

(1) N different samples are set by (X_i, t_i), where $X_i = [x_{i1}, x_{i2}, \ldots, x_{in}]^T \in R^n$, $t_i = [t_{i1}, t_{i2}, \ldots, t_{in}]^T \in R^m$. The infinitely differentiable activation function of the hidden layer neuron is $g(x)$, which can be described as:

$$\sum_{i=1}^{N} \beta_i g(W_i \cdot x_j + b_j) = o_j, \quad j = 1, 2, \ldots, N \tag{5}$$

where β_{in} is the connection weight of the i_{th} hidden layer neuron and n_{th} output layer neuron, $\beta_i = [\beta_{i1}, \beta_{i2}, \ldots, \beta_{in}]^T$. w_{in} is the connection weight of the i_{th} hidden layer neuron and the n_{th} input layer neuron, $W_i = [w_{i1}, w_{i2}, \ldots, w_{in}]$. b_j is the threshold of the j_{th} neuron on the hidden layer.

(2) The purpose of SLFN is to minimize the output error. Thus, W_i and b_i enable the result to approach to the t_j:

$$\sum_{i=1}^{N} \beta_i g(W_i \cdot x_j + b_i) = t_j, \quad j = 1, 2, \ldots, N \tag{6a}$$

$$H(W_1, \ldots, W_L, b_1, \ldots, b_L, X_1, \ldots, X_L) = \begin{bmatrix} g(W_1 \cdot X_1 + b_1) & \ldots & g(W_L \cdot X_1 + b_L) \\ \vdots & \ldots & \vdots \\ g(W_1 \cdot X_N + b_1) & \ldots & g(W_L \cdot X_N + b_L) \end{bmatrix} \tag{6b}$$

$$\beta = \begin{bmatrix} \beta_1^T \\ \vdots \\ \beta_L^T \end{bmatrix}_{L \times M}, \quad T = \begin{bmatrix} T_1^T \\ \vdots \\ T_2^T \end{bmatrix}_{N \times M} \tag{6c}$$

where H is the output matrix of the neuron on the hidden layer.

(3) The output weights are able to be acquired by settling the least square solution of next formula:

$$||H\beta - T|| = \min_{\beta} ||H\beta - T|| \tag{7a}$$

The solution is:

$$\hat{\beta} = H^{+}T \tag{7b}$$

where H^+ is the Moore-Penrose generalized inverse of output matrix.

C. RANDOM FOREST

RF refers to an ensemble learning method that employs random growing trees to classify and predict [43], also termed as random decision trees. The combination of Bagging and random subspace addresses the weaknesses of single tree, which is suitable for the classification of high dimensional data [44]. When RF is applied to classification, every decision tree is performed to categorize the samples. The final category is determined by the category winning the most votes. As for regression, the final result is obtained by the mean of the predicted values of the decision trees [45]. Because of speediness and efficiency, this algorithm has progressed in data mining. The detailed descriptions are as follows:

(1) Bootstrap is adopted to produce T training sets: $S_1, S_2, \ldots, S_T$, at random.
(2) The decision tree $D_1, D_2, \ldots, D_T$ is set up according to the correspond training set. m attributes are randomly screened from M attributes in a decision tree to compose a split attribute set. And the best attribute is selected as the splitting of the node.
(3) Pruning is not permitted when the trees grow.
(4) For the test set x, each decision tree is employed to acquire the category $D_1(x), D_2(x), \ldots, D_T(x)$.
(5) The output result is the mean of all predicted values of decision trees.

D. SUPPORT VECTOR MACHINE

As a model of machine learning, SVM makes striking progresses in pattern classification and regression analysis since proposed by Vapnik in 1964 [46]. The main theory is that a hyperplane is instituted to separate two types of data for the maximum interval. As for the nonlinear data, the nonlinear transformation is utilized to convert the input space into a high dimensional space, and the linear classification and optimal hyperplane could be completed [47]. The nonlinear transformation is accomplished by kernel function, such as linear function and polynomial function [48]. The following steps can express the concrete processing:

(1) Set the training set: $T = \{(x_1, y_1), \ldots, (x_i, y_i)\}(X \times Y)^l$, where $x_i \in X = R^n$ is the eigenvector, $y_i \in Y = \{1, -1\}(i = 1, 2, \ldots, l)$. The hyperplane is expressed as: $\omega \cdot x + b = 0$. Where ω is the weight vector, and b is the threshold.
(2) In order to maximize the margin of each category, the optimization of hyperplane is solved under the following condition:

$$\begin{cases} \min \phi(\omega) = \dfrac{1}{2}||\omega||^2 \\ s.t.\ y_i(\omega \cdot x_i + b) - 1 \geq 0, \quad i = 1, \ldots, n \end{cases} \tag{8}$$

(3) By introducing Lagrange multipliers a_i and a_i^*, the solution to the optimal classification plane is converted into the corresponding dual problem:

$$\max \sum_{i=1}^{n} a_i - \frac{1}{2} \sum_{i=1}^{n} \sum_{j=1}^{n} a_i a_j y_i y_j (x_i \cdot x_j) \tag{9a}$$

$$S.t. \begin{cases} 0 \leq a_i \leq c, \quad i = 1, \ldots, n \\ \sum_{i=1}^{n} a_i y_i = 0 \end{cases} \tag{9b}$$

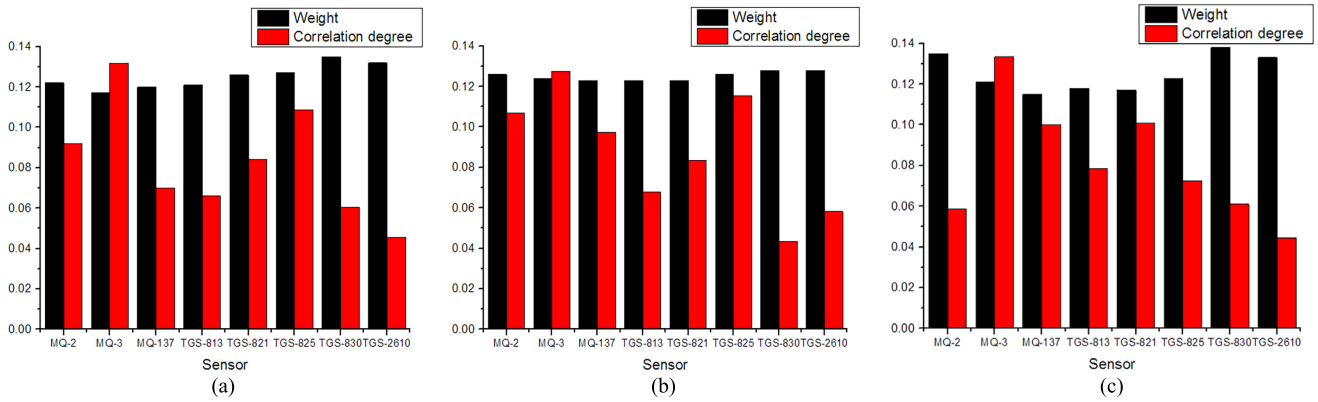

FIGURE 4. The weight of each sensor reacting with three kinds of ABS, (a) High heat-resistant ABS, (b) Heat-resistant ABS, (c) Flame-retardant ABS.

where c is the penalty parameter to measure the error of the model. The optimal solution is:

$$\begin{cases} a^* = (a_1^*, \ldots, a_n^*)^T \\ b* = y_i - \sum_{i=1}^{n} y_i a_i^* K(x_i - x_j) \end{cases} \tag{10}$$

(4) In this paper, the radial basis function is selected as the kernel function:

$$K(x, x_i) = \exp(-g||x - x_i||^2), \quad g > 0 \tag{11}$$

where g is the kernel function parameter, concerned with the data distribution of feature space. The decision function can be described as:

$$\begin{aligned} f(x) &= sgn\{\sum_{i=1}^{n} a_i^* y_i K(x_i \cdot x) + b^*\} \\ &= sgn\{\sum_{i=1}^{n} a_i^* y_i \exp(-g||x - x_i||^2) + b^*\} \end{aligned} \tag{12}$$

IV. RESULTS AND DISCUSSION

A. QUANTIFICATION OF ODOR INTENSITY

According to GRA, the referred sequence is often the optimal sequence [49]. Compared with other sensors, MQ-2 and MQ-3 were equipped with striking response values. However, the response curves of MQ-2 were steadier than that of MQ-3 in the stable state. Therefore, the feature of MQ-2 was selected as the referred sequence. And the features of the other sensors were served as the compared sequences. As shown in Fig. 4, the correlation degree of each sensor was distinct from one another, which revealed the better contribution of the sensors in the array. The final quantified results are shown in Fig. 5. The quantified values of odor intensity were becoming greater with the increase in the weight of ABS, which conformed with the fact that the odor is becoming more intense with the increased concentration. Besides, the odor intensity of different ABS brands was evidently differentiated by the quantified numbers under the same weight. From the above, the odor intensity of ABS could be quantified by the odor evaluation system. The odor of high heat resistant ABS was more intense than that of others, and the odor of flame-retardant ABS was the weakest.

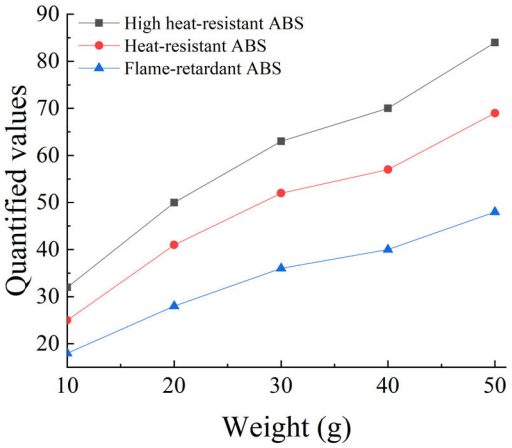

FIGURE 5. The quantified results of odor intensity from three kinds of ABS.

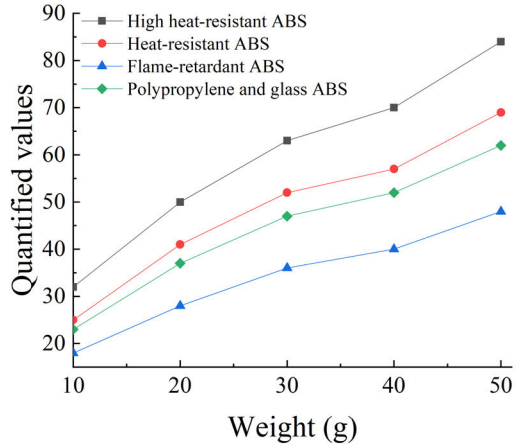

FIGURE 6. The contrast of the quantified values between polypropylene and glass ABS and other types.

TABLE 6. Comparison of the regression results of four kinds of ABS by ELM.

Types of ABS	Training Set		Test Set	
	R^2	RMSE	R^2	RMSE
High heat-resistant ABS	0.9771	0.2974	0.9635	0.3707
Heat-resistant ABS	0.9872	0.0135	0.9745	0.2022
Flame-retardant ABS	0.9607	0.2849	0.9442	0.3927
Polypropylene and glass ABS	0.9278	0.4065	0.9243	0.5187

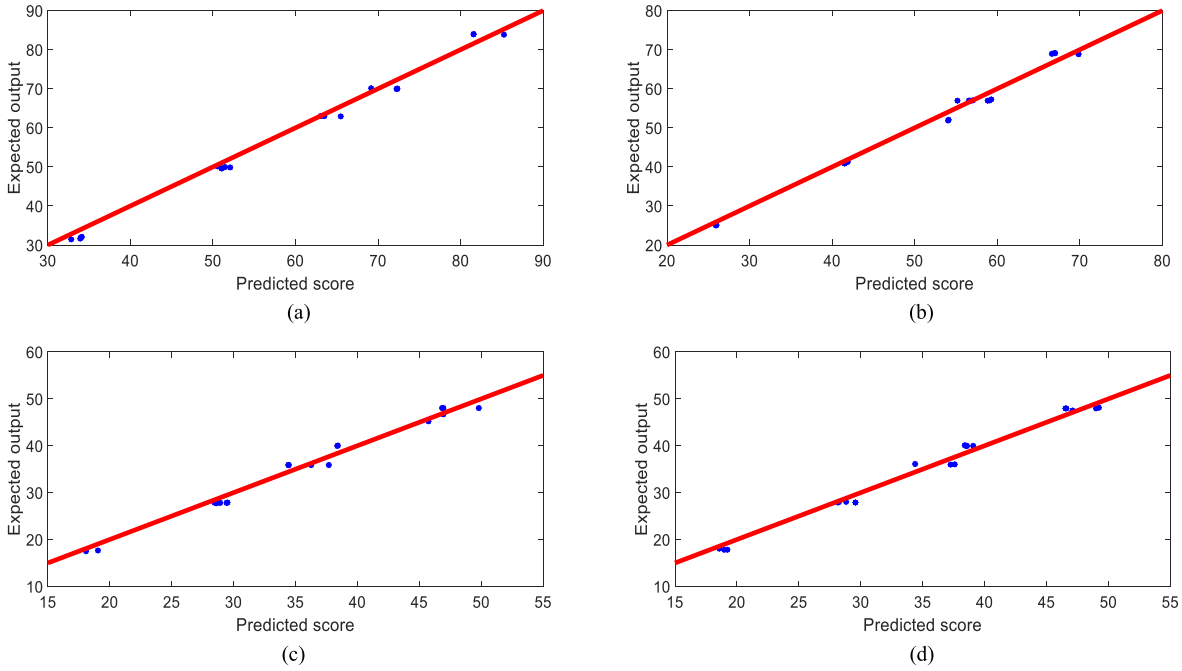

FIGURE 7. The fitting effect of the predicted values and the quantified values of four kinds of ABS: (a) High heat-resistant ABS, (b) Heat-resistant ABS, (c) Flame-retardant ABS, (d) Polypropylene and glass ABS.

To verify the above results, polypropylene and glass ABS, an extra brand of ABS, was measured by the odor evaluation system. As shown in Fig. 6, the quantified values of polypropylene and glass ABS were also getting greater with the increase in the weight of ABS. Besides, the odor intensity of polypropylene and glass ABS was distinguished from that of other brands when the samples were equipped with the same weight.

B. QUANTITATIVE REGRESSION OF ODOR INTENSITY

The regression models were constructed by ELM, RF, and SVM. For each brand, 60 groups of data were selected as the training set at random, and the remaining 20 groups of data were used as the test set. The input of the model was composed of the features of the odor and the output was made up of the quantified values of odor intensity. In order to describe the predicted performance of the models, the R^2 and the RMSE were introduced. The R^2 is termed as coefficient of determination, used to measure the fitting effect of the regression model. In general, the larger R^2 between [0, 1] means the better fitting effect. The RMSE, namely root mean square error, is served as an indicator to evaluate the deviation between the predicted values and observed values.

1) REGRESSION ANALYSIS BY ELM

The regression model was constructed by ELM, where the number of neurons was 20. As shown in Table 6, the $R^2 > 0.92$ in the training sets and the test sets, and the difference of R^2 between the training sets and the corresponding test sets was less than 0.02. Therefore, ELM possessed good universality and generalization for four kinds of ABS. Besides, the quantified values of heat-resistant ABS were predicted well in the training sets ($R^2 > 0.98$) and the test sets ($R^2 > 0.97$). The fitting effect of the predicted values and the quantified values in the test sets is shown in Fig. 7.

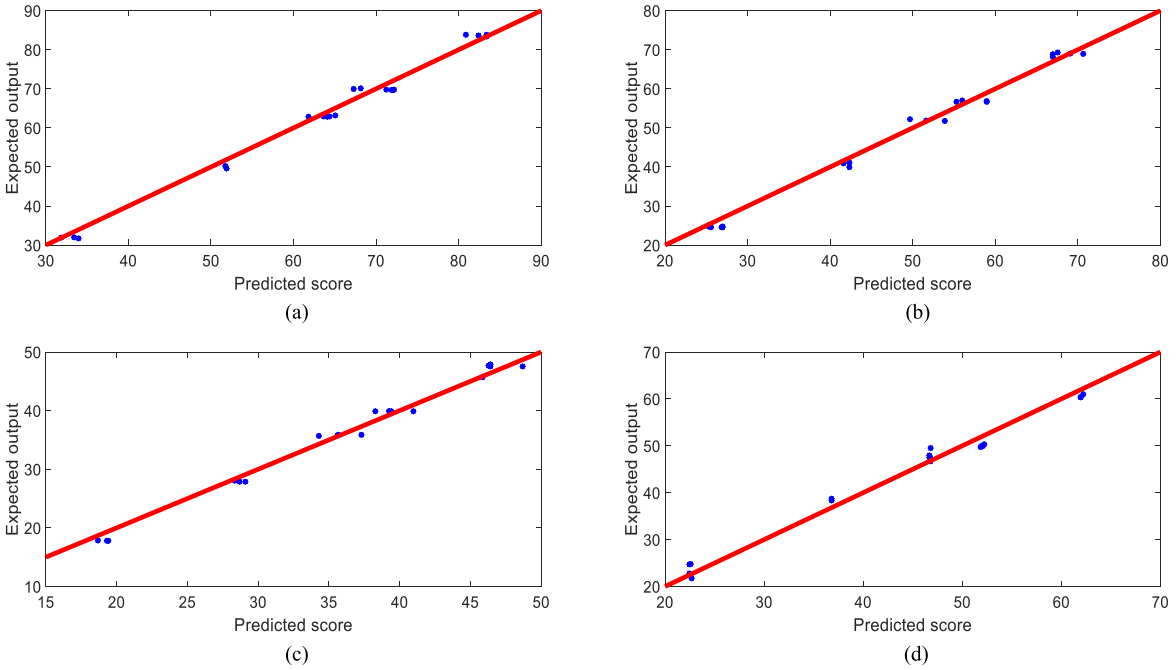

FIGURE 8. The fitting effect of the predicted values and the quantified values of four kinds of ABS: (a) High heat-resistant ABS, (b) Heat-resistant ABS, (c) Flame-retardant ABS, (d) Polypropylene and glass ABS.

TABLE 7. Comparison of the regression results of four kinds of ABS by RF.

Types of ABS	Training Set		Test Set	
	R^2	RMSE	R^2	RMSE
High heat-resistant ABS	0.9172	0.3458	0.8972	0.4893
Heat-resistant ABS	0.9214	0.3185	0.9035	0.8324
Flame-retardant ABS	0.9649	0.5723	0.9542	0.5928
Polypropylene and glass ABS	0.9973	0.4372	0.9853	0.5346

TABLE 8. Comparison of the regression results of four kinds of ABS by SVM.

Types of ABS	Best Parameter		Training Set		Test Set	
	c	g	R^2	RMSE	R^2	RMSE
High heat-resistant ABS	157.412	0.0912	0.9806	0.0431	0.9273	0.1273
Heat-resistant ABS	2.479	0.164	0.9872	0.0135	0.8872	0.2022
Flame-retardant ABS	5.736	0.0932	0.9974	0.1832	0.9462	0.3927
Polypropylene and glass ABS	36.153	0.1527	0.9976	0.0063	0.9613	0.4381

2) REGRESSION ANALYSIS BY RF

In RF, the number of the decision trees was 500, and the number of attributes in the split attribute set was 5. Table 7 shows the regression results of four kinds of ABS. It can be seen that the training sets with $R^2 > 0.91$ and the test sets with $R^2 > 0.89$. And the difference of R^2 between the training sets and the corresponding test sets in ELM was less than that in RF, which proved that ELM was better at applicability and generalization. Among four kinds of ABS, the quantified values of polypropylene and glass ABS were predicted better, with $R^2 > 0.99$ in the training sets and $R^2 > 0.98$ in the test sets. Fig. 8 shows the fitting effect

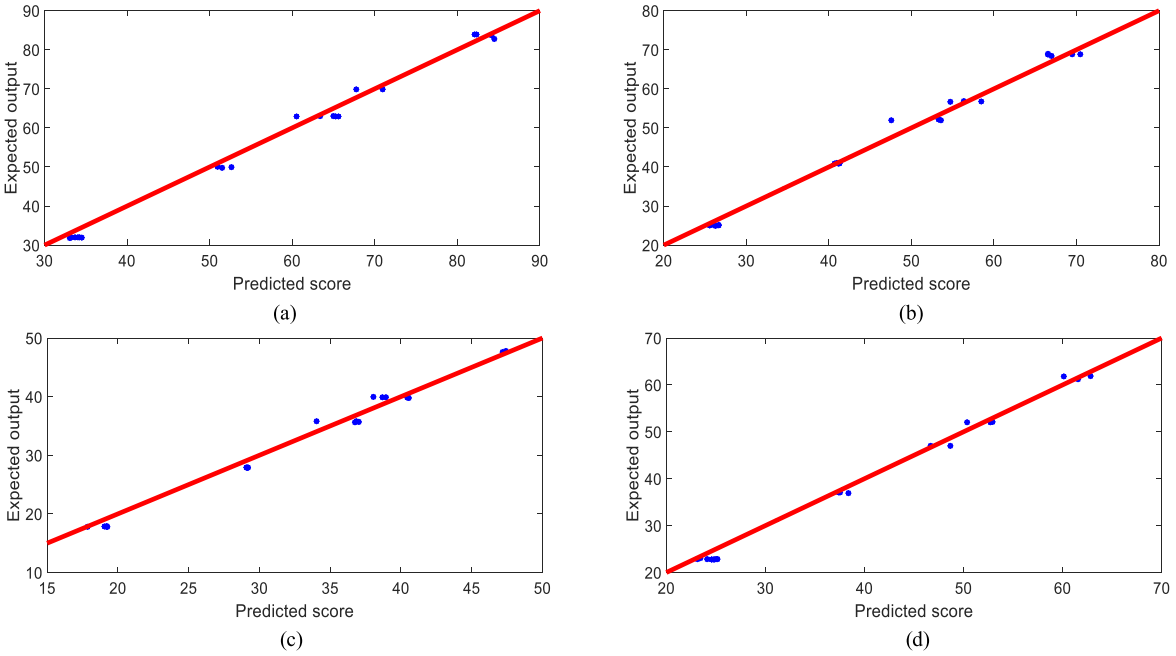

FIGURE 9. The fitting effect of the predicted values and the quantified values of four kinds of ABS: (a) High heat-resistant ABS, (b) Heat-resistant ABS, (c) Flame-retardant ABS, (d) Polypropylene and glass ABS.

of the predicted values and the quantified values in the test sets.

3) REGRESSION ANALYSIS BY SVM

The Cuckoo Search (CS) was employed to search the best parameters (c and g). And the mean square error was utilized as the fitness function. As shown in Table 8, SVM had a preferable presentation in the training sets ($R^2 > 0.98$) but not the test sets ($0.88 < R^2 < 0.97$). The difference of R^2 between the training sets and the corresponding test sets in SVM was greater than that in the other models, which certified that SVM was provided with inferior fitting. The quantified values of polypropylene and glass ABS were also predicted well by SVM, with $R^2 > 0.99$ in the training sets and $R^2 > 0.96$ in the test sets. The fitting effect of the predicted values and the quantified values in the test sets is shown in Fig. 9.

V. CONCLUSION

In this paper, an odor evaluation system was developed to detect the odor intensity of four kinds of ABS. Eight sensors were selected to compose an array. Then, the data preprocessing and the feature extraction were applied to deal with the data of smells. Finally, the correlations and the weights of different sensors were obtained to quantify the odor intensity. According to the quantified consequences, ELM, RF, and SVM were introduced to construct the regression models. The particular conclusions are as follows:

(1) Design of the ABS odor evaluation system: the system included a sampling device, a sensor array, and an analysis software. Eight sensors were screened by CV, ANOVA, and PCA to construct an array with stability, repeatability, and selectivity.

(2) Quantification of the odor intensity: the quantified values were becoming greater with the increase in the weight of ABS and discriminated the odor intensity of four kinds of ABS correctly. Among four kinds of ABS, the high heat-resistant ABS with the maximum odor and the flame-retardant ABS with the minimum odor.

(3) Construction of the regression models: ELM was equipped with the better universality ($R^2 > 0.92$), however, SVM was a suboptimal choice in fitting. The quantified values of polypropylene and glass ABS were predicted well by RF and SVM, and the quantified values of heat-resistant ABS were predicted well by ELM.

This study indicated that the odor evaluation system could perceive the smells of four kinds of ABS and quantify their severity, offering a novel technique for the evaluation of the odor intensity. Thus, this system was likely to substitute human evaluation in the field of automobiles.

REFERENCES

[1] B. Xu, X. Chen, and J. Xiong, "Air quality inside motor vehicles' cabins: A review," *Indoor Built Environ.*, vol. 27, no. 4, pp. 452–465, Apr. 2018.

[2] M. F. Hazlehurst, E. W. Spalt, T. P. Nicholas, C. L. Curl, M. E. Davey, G. L. Burke, K. E. Watson, S. Vedal, and J. D. Kaufman, "Contribution of the in-vehicle microenvironment to individual ambient-source nitrogen dioxide exposure: The multi-ethnic study of atherosclerosis and air pollution," *J. Exposure Sci. Environ. Epidemiol.*, vol. 28, no. 4, pp. 371–380, Jun. 2018.

[3] A. Kadiyala and A. Kumar, "Development and application of a methodology to identify and rank the important factors affecting in-vehicle particulate matter," *J. Hazardous Mater.*, vols. 213–214, pp. 140–146, Apr. 2012.

[4] Y.-Y. Lu, Y. Lin, H. Zhang, D. Ding, X. Sun, Q. Huang, L. Lin, Y.-J. Chen, Y.-L. Chi, and S. Dong, "Evaluation of volatile organic compounds and carbonyl compounds present in the cabins of newly produced, medium- and large-size coaches in China," *Int. J. Environ. Res. Public Health*, vol. 13, no. 6, p. 596, Jun. 2016.
[5] World Health Organization, "Reducing risks, promoting healthy life," Educ. Health, Abingdon, U.K., World Health Rep. 2002, 2003, p. 230, vol. 16, no. 16.
[6] Y.-C. Chien, "Variations in amounts and potential sources of volatile organic chemicals in new cars," *Sci. Total Environ.*, vol. 382, nos. 2–3, pp. 228–239, Sep. 2007.
[7] J. Li, R. D. Hodges, R. Gutierrez-Osuna, G. Luckey, J. Crowell, S. S. Schiffman, and H. T. Nagle, "Odor assessment of automobile cabin air with field asymmetric ion mobility spectrometry and photoionization detection," *IEEE Sensors J.*, vol. 16, no. 2, pp. 409–417, Jan. 2016.
[8] X. Han, G. Wang, Y. He, Y. Wang, Y. Qiao, and L. Zhang, "Surface modification of ABS with Cr6+ free etching process in the electroless plating," *J. Adhes. Sci. Technol.*, vol. 32, no. 22, pp. 2481–2493, Nov. 2018.
[9] X. Han, G. Wang, J. He, J. Guan, and Y. He, "Influence of temperature on the surface property of ABS resin in $KMnO_4$ etching solution," *Surf. Interface Anal.*, vol. 51, no. 2, pp. 177–183, Feb. 2019.
[10] F. S. Kamelian, E. Saljoughi, P. Shojaee Nasirabadi, and S. M. Mousavi, "Modifications and research potentials of acrylonitrile/butadiene/styrene (ABS) membranes: A review," *Polym. Compos.*, vol. 39, no. 8, pp. 2835–2846, Aug. 2018.
[11] J. Faber, K. Brodzik, A. Gołda-Kopek, and D. Łomankiewicz, "Benzene, toluene and xylenes levels in new and used vehicles of the same model," *J. Environ. Sci.*, vol. 25, no. 11, pp. 2324–2330, Nov. 2013.
[12] O. V. Monogarova, K. V. Oskolok, and V. V. Apyari, "Colorimetry in chemical analysis," *J. Anal. Chem.*, vol. 73, no. 11, pp. 1076–1084, 2018.
[13] J. Xu, W. Su, Z. Li, W. Liu, S. Liu, and X. Ding, "A modularized and flexible sensor based on MWCNT/PDMS composite film for on-site electrochemical analysis," *J. Electroanal. Chem.*, vol. 806, pp. 68–74, Dec. 2017.
[14] P. Q. Tranchida, F. A. Franchina, P. Dugo, and L. Mondello, "Comprehensive two-dimensional gas chromatography-mass spectrometry: Recent evolution and current trends," *Mass Spectrometry Rev.*, vol. 35, no. 4, pp. 524–534, Jul. 2016.
[15] P. Q. Tranchida, G. Purcaro, M. Maimone, and L. Mondello, "Impact of comprehensive two-dimensional gas chromatography with mass spectrometry on food analysis," *J. Separat. Sci.*, vol. 39, no. 1, pp. 149–161, Jan. 2016.
[16] *Determination-of-Formaldehyde-From-Vehicle-Interior-With-Modif*, document VDA270, 1992.
[17] *Test Method for Determining the Resistance to Odour Propagation of trim Materials*, document GME 60276, 2000.
[18] *Smell Quality Of Non-Metallic Materials*, document TSM0505G, 2007.
[19] M. Verriele, "Odor evaluation and discrimination of car cabin and its components: Application of the 'field of odors' approach in a sensory descriptive analysis," *J. Sensory Stud.*, vol. 27, no. 2, pp. 102–110, 2012.
[20] J. Li, R. Gutierrez-Osuna, R. D. Hodges, G. Luckey, J. Crowell, S. S. Schiffman, and H. T. Nagle, "Using field asymmetric ion mobility spectrometry for odor assessment of automobile interior components," *IEEE Sensors J.*, vol. 16, no. 14, pp. 5747–5756, Jul. 2016.
[21] K. J. Johnson and S. L. Rose-Pehrsson, "Sensor array design for complex sensing tasks," *Annu. Rev. Anal. Chem.*, vol. 8, no. 1, pp. 287–310, Jul. 2015.
[22] C. Kong, S. Zhao, X. Weng, C. Liu, R. Guan, and Z. Chang, "Weighted summation: Feature extraction of farm pigsty data for electronic nose," *IEEE Access*, vol. 7, pp. 96732–96742, 2019.
[23] Y. Shi, F. Gong, M. Wang, J. Liu, Y. Wu, and H. Men, "A deep feature mining method of electronic nose sensor data for identifying beer olfactory information," *J. Food Eng.*, vol. 263, pp. 437–445, Dec. 2019.
[24] X. Pan, H. Zhang, W. Ye, A. Bermak, and X. Zhao, "A fast and robust gas recognition algorithm based on hybrid convolutional and recurrent neural network," *IEEE Access*, vol. 7, pp. 100954–100963, 2019.
[25] M. T. Kalit, "Application of electronic nose and electronic tongue in the dairy industry," *Mljekarstvo*, vol. 64, no. 4, pp. 228–244, 2014.
[26] Y. Yin, H. Yu, B. Chu, and Y. Xiao, "A sensor array optimization method of electronic nose based on elimination transform of Wilks statistic for discrimination of three kinds of vinegars," *J. Food Eng.*, vol. 127, pp. 43–48, Apr. 2014.
[27] B. Szulczyński, K. Armiński, J. Namieśnik, and J. Gębicki, "Determination of odour interactions in gaseous mixtures using electronic nose methods with artificial neural networks," *Sensors*, vol. 18, no. 2, p. 519, Feb. 2018.
[28] S. Osowski and K. Siwek, "Mining data of noisy signal patterns in recognition of gasoline bio-based additives using electronic nose," *Metrol. Meas. Syst.*, vol. 24, no. 1, pp. 27–44, Mar. 2017.
[29] H. Men, S. Fu, J. Yang, M. Cheng, Y. Shi, and J. Liu, "Comparison of SVM, RF and ELM on an electronic nose for the intelligent evaluation of paraffin samples," *Sensors*, vol. 18, no. 1, p. 285, Jan. 2018.
[30] L. Xu, J. He, S. Duan, X. Wu, and Q. Wang, "Comparison of machine learning algorithms for concentration detection and prediction of formaldehyde based on electronic nose," *Sensor Rev.*, vol. 36, no. 2, pp. 207–216, Mar. 2016.
[31] H. Men, Y. Jiao, Y. Shi, F. Gong, Y. Chen, H. Fang, and J. Liu, "Odor fingerprint analysis using feature mining method based on olfactory sensory evaluation," *Sensors*, vol. 18, no. 10, p. 3387, Oct. 2018.
[32] H. Men, Y. Shi, S. Fu, Y. Jiao, Y. Qiao, and J. Liu, "Mining feature of data fusion in the classification of beer flavor information using E-tongue and E-nose," *Sensors*, vol. 17, no. 7, p. 1656, Jul. 2017.
[33] H. Men, Y. Shi, Y. Jiao, F. Gong, and J. Liu, "Electronic nose sensors data feature mining: A synergetic strategy for the classification of beer," *Anal. Methods*, vol. 10, no. 17, pp. 2016–2025, Apr. 2018.
[34] S. Liu, "On the new model system and framework of grey system theory," *J. Grey Syst.*, vol. 28, no. 1, pp. 1–15, 2016.
[35] K. Deng, B. Meng, and C. Xiang, "Adaptability to stratum characteristics for layout of thrust system in tunneling machines based on variation coefficient," *Adv. Mech. Eng.*, vol. 8, no. 12, Dec. 2016, Art. no. 168781401668243.
[36] B. Zawieja and A. Szczepańska-Álvarez, "A simulation study of the Bennett test and Miller test for coefficients of variation," *Commun. Statist.-Simul. Comput.*, vol. 46, no. 5, pp. 3701–3711, Nov. 2015.
[37] Y. Wang, Y. Huang, X. Zeng, G. Wei, J. Zhou, T. Fang, and H. Chen, "Faulty feeder detection of single phase-earth fault using grey relation degree in resonant grounding system," *IEEE Trans. Power Del.*, vol. 32, no. 1, pp. 55–61, Feb. 2017.
[38] G. Sun and H. Zhu, "Characteristic parameter extraction of running-in attractors based on phase trajectory and grey relation analysis," *Nonlinear Dyn.*, vol. 95, no. 4, pp. 3115–3126, Mar. 2019.
[39] R. Zhu, P. Zhou, C. Q. Zhou, and J. Li, "Fuzzy grey relational analysis for influencing factors of heat transfer in a blast furnace hearth," *Ironmaking Steelmaking*, vol. 45, no. 10, pp. 899–906, Nov. 2018.
[40] G.-B. Huang, H. Zhou, X. Ding, and R. Zhang, "Extreme learning machine for regression and multiclass classification," *IEEE Trans. Syst., Man, Cybern. B. Cybern.*, vol. 42, no. 2, pp. 513–529, Apr. 2012.
[41] G.-B. Huang, Q.-Y. Zhu, and C.-K. Siew, "Extreme learning machine: Theory and applications," *Neurocomputing*, vol. 70, nos. 1–3, pp. 489–501, Dec. 2006.
[42] S. Ding, X. Xu, and R. Nie, "Extreme learning machine and its applications," *Neural Comput. Appl.*, vol. 25, nos. 3–4, pp. 549–556, Sep. 2014.
[43] E. Scornet, "Random forests and kernel methods," *IEEE Trans. Inf. Theory*, vol. 62, no. 3, pp. 1485–1500, Mar. 2016.
[44] M. E. H. Daho and M. A. Chikh, "Combining bootstrapping samples, random subspaces and random forests to build classifiers," *J. Med. Imag. Health Inf.*, vol. 5, no. 3, pp. 539–544, Jun. 2015.
[45] J. W. Coulston, C. E. Blinn, V. A. Thomas, and R. H. Wynne, "Approximating prediction uncertainty for random forest regression models," *Photogramm. Eng. Remote Sens.*, vol. 82, no. 3, pp. 189–197, Mar. 2016.
[46] A. T. Azar and S. A. El-Said, "Performance analysis of support vector machines classifiers in breast cancer mammography recognition," *Neural Comput. Appl.*, vol. 24, no. 5, pp. 1163–1177, Apr. 2014.
[47] S. Ding, H. Huang, J. Yu, and H. Zhao, "Research on the hybrid models of granular computing and support vector machine," *Artif. Intell. Rev.*, vol. 43, no. 4, pp. 565–577, Apr. 2015.
[48] H. Ju, Q. Hou, and L. Jing, "Fuzzy and interval-valued fuzzy non-parallel support vector machine," *J. Intell. Fuzzy Syst.*, vol. 36, no. 3, pp. 2677–2690, Mar. 2019.
[49] Y. Kuo, T. Yang, and G.-W. Huang, "The use of grey relational analysis in solving multiple attribute decision-making problems," *Comput. Ind. Eng.*, vol. 55, no. 1, pp. 80–93, Aug. 2008.

HONG MEN was born in China, in 1973. He received the master's degree in power system and automation from Northeast Electric Power University, Jilin, in 2002, and the Ph.D. degree in biomedical engineering from Zhejiang University, Hangzhou, in 2005.

From 2005 to 2008, he was a Lecturer with the Department of Instrument Science and Technology, Northeast Electric Power University. Since 2013, he has been a Professor with the Department of Instrument Science and Technology, Northeast Electric Power University. He is the author of more than 80 articles. His research interests include sensor fabrication, electeonic nose, machine perception technology, EEG, pattern recognition, and intelligent detection.

CHONGBO YIN was born in Jilin, China. He received the bachelor's degree from Northeast Electric Power University, in 2018, where he is currently pursing master's degree. His research direction is eletronic nose.

YAN SHI was born in Jilin, China. He received the master's degree from Northeast Electric Power University, in 2018, where he is currently pursing Ph.D. degree. His research interests include machine perception technology and pattern recognition.

XIAOTONG LIU was born in Jilin, China. She received the bachelor's degree from the North China University of Technology. She is currently pursuing the master's degree with Northeast Electric Power University. Her research direction is olfactory EEG.

HAIRUI FANG was born in Inner Mongolia, China, in 1989. He received the Ph.D. degree from Jilin University, in 2017. He is currently an Associate Professor and a master's Tutor with the School of Automation Engineering, Northeast Electric Power University. His main research interests include development of sensitive device and instrument, detection, and application for weak signal.

XIAOJU HAN was born in Liaoning, China, in 1981. She received the Ph.D. degree from Northeastern University. She is currently a Lecturer with the School of Automation Engineering, Northeast Electric Power University. Her research interests include application of RFID technology in supply chain management and line sensor network applications.

JINGJING LIU was born in Jilin, China, in 1986. She received the Ph.D. degree in agricultural electrification and automation from Jilin University. Since 2013, she has been an Associate Professor and a master's Tutor with the School of Automation Engineering, Northeast Electric Power University. She is the author of over 30 articles and holds four patents. Her main research interests include sensor array construction, multisensor data fusion, and evaluation of sensory information.